



Article

# Enhancing Organic Contaminant Removal from Wool Scouring Wastewater Using Chemically Modified Biochars

Simeng Li \* , Desarae Tasnady, Shannon Skelley, Blanca Calderon and Sherine Jiang

Department of Civil Engineering, College of Engineering, California State Polytechnic University, Pomona, 3801 West Temple Avenue, Pomona, CA 91768, USA; datasnady@cpp.edu (D.T.); smskelley@cpp.edu (S.S.); bcalderon@cpp.edu (B.C.); syjjj161@gmail.com (S.J.)

\* Correspondence: sli@cpp.edu; Tel.: +1-909-869-4787

**Abstract:** In recent times, biochar has emerged as a promising and sustainable solution for COD reduction in wastewater treatment. This study explores the potential of chemically modified biochars as efficient adsorbents for the removal of organic contaminants, specifically oils, fats, and grease (OFG), from wool scouring wastewater. Proximate analysis revealed distinct properties among the biochars, with KOH-treated biochar demonstrating the most promising characteristics, including lower volatile matter, higher fixed carbon content, and reduced ash content, indicating a stable and carbon-rich structure. A meticulous examination of the KOH-treated biochar's surface characteristics revealed the presence of elevated carbon and nitrogen content, complemented by an expansive surface area measuring 724.4 m<sup>2</sup>/g. This surface area was at least twice as extensive as that observed in the other post-treated biochar samples. The kinetic adsorption of COD and soluble COD was well fitted by the pseudo-first-order model, with equilibrium achieved in approximately 200 min. The KOH-treated biochar exhibited the highest equilibrium adsorption capacities for both COD and soluble COD in both Dorset wool (Dorset) and Bluefaced Leicester (BFL) wastewater, highlighting its efficacy in OFG removal. Despite these promising results, further research is needed to explore biochar's surface characteristics, pore structure, and performance under diverse conditions, as well as its integration with existing treatment processes and potential for regeneration and reuse. This study contributes to advancing sustainable wastewater treatment methods using chemically modified biochars.

**Keywords:** biochar; wool scouring wastewater; surface modification; COD; soluble COD; elemental analysis; proximate analysis; adsorption kinetic model; surface characterization



**Citation:** Li, S.; Tasnady, D.; Skelley, S.; Calderon, B.; Jiang, S. Enhancing Organic Contaminant Removal from Wool Scouring Wastewater Using Chemically Modified Biochars. *C* **2024**, *10*, 6. <https://doi.org/10.3390/c10010006>

Academic Editor: Miguel A. Montes Morán

Received: 11 October 2023

Revised: 30 December 2023

Accepted: 3 January 2024

Published: 5 January 2024



**Copyright:** © 2024 by the authors. Licensee MDPI, Basel, Switzerland. This article is an open access article distributed under the terms and conditions of the Creative Commons Attribution (CC BY) license (<https://creativecommons.org/licenses/by/4.0/>).

## 1. Introduction

Wool scouring wastewater, a byproduct of the textile industry, represents a complex and environmentally consequential effluent stream originating from the cleaning and processing of raw wool fibers. This wastewater is characterized by high organic content, including fats, oils, and lanolin, as well as suspended solids and alkaline pH levels [1,2]. The environmental repercussions of untreated or inadequately treated wool scouring wastewater are substantial, including water pollution, soil degradation, and adverse effects on aquatic ecosystems [3,4]. These contaminants can compromise water quality, disrupt microbial communities, and potentially harm sensitive aquatic species [4,5]. Furthermore, the challenges associated with wool scouring wastewater management are multifaceted, ranging from the development of efficient treatment technologies capable of handling its unique composition to addressing the economic and regulatory considerations that surround its disposal and reuse within a sustainable textile industry framework [6–8].

Owing to the substantial levels of oils, fats, grease (OFG), and intricate compounds found in wool scouring wastewater, conventional biological wastewater treatment processes such as activated sludge, anaerobic digestion, and aerobic decomposition, which are

traditionally employed for organic pollutant biodegradation, often encounter challenges, resulting in incomplete degradation and the emergence of unpleasant odor concerns [6,9]. On the other hand, chemical and physical treatment processes such as coagulation and flocculation use chemical agents such as aluminum or iron salts to facilitate the aggregation and settling of suspended solids [10]. However, excessive chemical use can generate large quantities of sludge and increase the overall environmental impact [10]. Technologies like ultrafiltration and reverse osmosis can effectively remove contaminants, but they are energy-intensive and may clog or foul membranes due to the high fouling potential of wool scouring wastewater [11,12]. Although activated carbon adsorption can be used to effectively remove organic contaminants, this method is costly and requires frequent regeneration and/or replacement of the adsorbent material [13]. To address these problems, ongoing research and development efforts are focused on innovative treatment technologies, process optimization, and the integration of cleaner production practices within the wool scouring industry to minimize the generation of problematic wastewater in the first place [6].

Engineered biochar presents a promising and sustainable approach for treating wool scouring wastewater, offering several advantages over traditional methods discussed earlier. Firstly, with its porous structure and high surface area, engineered biochar can provide a favorable environment for beneficial microorganisms to thrive [14]. It promotes microbial activity and can serve as a substrate for biofilm formation, facilitating the breakdown of recalcitrant organic pollutants more effectively than conventional biological treatments [14]. Moreover, biochar can be modified to enhance its adsorption capabilities [15], effectively removing organic contaminants and suspended solids from the wastewater without the need for large quantities of chemical coagulants. This reduces the production of chemical sludge, which is often a problem associated with traditional methods [16]. Furthermore, biochar-based treatment systems can be integrated into sustainable, closed-loop approaches, offering the potential for resource recovery [15]. Biochar can serve as a valuable soil conditioner or be regenerated for repeated use in wastewater treatment, minimizing waste generation and promoting environmental sustainability [17]. Additionally, engineered biochar can be tailored to specific wastewater characteristics, making it a versatile solution for the diverse composition of wool scouring wastewater [15]. Its versatility and adaptability make it a promising technology to address the variability in pollutant loads that wool scouring facilities may encounter.

The efficiency of adsorption processes hinges significantly upon the characteristics of biochar, including surface area, pore structure, and functional group types [18,19]. Therefore, the modification of biochar is essential to broaden its range of applications. Common methods for achieving this modification are categorized into chemical and physical approaches. Chemical modification encompasses acid-, alkalinity-, oxidizing agent-, and metal-based modifications [20,21], while physical modification primarily involves techniques like ball milling and gas purging [21,22]. Among these, chemical activation methods have gained widespread acceptance due to their advantages, including low activation temperature, brief activation duration, high specific surface area, and the ability to control pore structure [20,23]. Potassium permanganate ( $\text{KMnO}_4$ ) is a frequently employed chemical activator known for its potent oxidation capabilities, enhancing the formation of oxygen-containing functional groups on biochar [24]. Furthermore,  $\text{KMnO}_4$  modification enhances biochars' surface binding capacity by generating a hierarchical porous structure [25]. In recent years, research has ventured into the utilization of biochar modified with  $\text{KMnO}_4$ , potassium hydroxide (KOH), and sulfuric acid ( $\text{H}_2\text{SO}_4$ ) in diverse wastewater treatment scenarios, including the removal of heavy metal ions and antibiotics [26–28]. Nonetheless, there is a notable scarcity of studies investigating the viability of employing biochar for the treatment of wool scouring wastewater.

This study seeks to assess the influence of various chemical agents in post-treatment on the efficiency of biochar in eliminating both soluble and insoluble organic contaminants from wool scouring wastewater. Concurrently, an innovative tea-bag style biochar ad-

sorption treatment approach has been devised, offering prospects for potential pilot-scale research in the future. Consequently, this investigation endeavors to furnish laboratory-derived evidence substantiating the effectiveness of this novel treatment method. With its cost-effectiveness and sustainability as an adsorbent, biochar holds the potential to treat wool scouring wastewater, facilitating potential reuse or alleviating the burden on subsequent treatment processes.

## 2. Materials and Methods

### 2.1. Pristine Biochar

In this study, we employed a commercially available biochar known for its cost-effectiveness, while its specific trade name remains undisclosed to uphold impartiality and avoid potential conflicts of interest. The pristine biochar underwent a grinding process, reducing it into fine powders with a mesh size of 16, carried out using a mortar and pestle.

### 2.2. Post-Treatment of Biochar

One of the four post-treatments of biochar involved its immersion in deionized (DI) water, with a biochar-to-water ratio of 1:10 (*wt./wt.*). This mixture underwent continuous agitation at 60 rpm for 24 h. Subsequently, the suspension was subjected to centrifugation at  $15,000 \times g$  for 20 min to separate the biochar from the supernatant water. Following this, the biochar was subjected to drying in an oven at 105 °C for 24 h and promptly stored in airtight containers. The other three post-treatments of the biochar followed a similar procedure, with DI water being substituted by 20% (*wt./wt.*) H<sub>2</sub>SO<sub>4</sub>, 2 M KOH solution, and 2 M KMnO<sub>4</sub> solution, respectively.

### 2.3. Synthetic Wool Scouring Wastewater

Dorset Horn wool and Bluefaced Leicester wool, sourced directly from Californian sheep farms, served as the primary materials for generating two distinct types of synthetic wool scouring wastewater, hereafter referred to as Dorset and BFL. In each wool washing cycle, a 100 g wool sample was placed within a 2 L container, followed by the addition of 1 L of tap water and 2 mL of detergent. The sealed container underwent vigorous shaking for a duration of 5 min, after which the liquid was drained into a 5-gallon container. Subsequently, the wool residue within the 2 L container was rinsed with 1 L of water to eliminate any remaining liquid residues. This wool sample underwent a total of 3 washing cycles, with the wastewater collected from these cycles constituting the synthetic wool scouring wastewater, which was later subjected to pH, electrical conductivity (EC), and chemical oxygen demand (COD) analysis. Notably, for the determination of its soluble COD (i.e., SCOD), the wastewater sample was filtered through a 0.22 µm syringe filter (Biomed Scientific, Miami, FL, USA) prior to analysis.

### 2.4. Biochar-Based COD Removal from Wastewater

A tea-bag style biochar adsorption treatment process was developed for the removal of COD from synthetic wool scouring wastewater. Following the post-treatment, 10 g of biochar were enclosed within a nylon cloth sachet and securely fastened to a metal component, allowing it to submerge to the midpoint of the 1 L wastewater in the cylindrical reactor. To facilitate gentle interaction between the pollutants and the biochar within the sachet, the wastewater was continuously agitated using a cylindrical magnetic stir bar (5 × 15 mm). At hydraulic retention times (HRTs) of 10, 30, 60, 90, 120, and 180 min, 6 mL wastewater samples were extracted for analysis. These collected wastewater samples were promptly preserved in a refrigerator at −20 °C prior to subsequent analysis. Three parallel replicates were carried out for each experimental condition.

### 2.5. Chemical Analysis

The wool scouring wastewater samples underwent analysis for EC, pH, COD, and SCOD. EC was determined using an electrical conductivity meter (HQ430D, Hach, Love-

land, CO, USA), while pH measurements were conducted using a pH meter (Lab 870, Schott Instruments, Mainz, Germany). COD levels in the wastewater were determined following the Hach method (TNT 822, Hach, Loveland, CO, USA). Notably, for the assessment of its SCOD, the wastewater sample was first filtered through a 0.22  $\mu\text{m}$  syringe filter (Biomed Scientific, Miami, FL, USA) before analysis.

### 2.6. Biochar Characterization

The biochar's carbon, hydrogen, nitrogen, and oxygen content were analyzed utilizing an ultimate analysis instrument (Vario Micro Cube, Elementar, Ronkonkoma, NY, USA). To ascertain the remaining oxygen content, a mass balance approach was employed following ash testing, calculated using the formula  $\text{O}\% = 100\% - \text{C}\% - \text{H}\% - \text{N}\% - \text{S}\% - \text{Ash}\%$ . Proximate analysis of the biochar was carried out following the procedures outlined in a previous study [29].

For the determination of the biochar's specific surface area, a Brunauer–Emmett–Teller (BET) surface analysis instrument (NOVA 4200e, Quantachrome Instruments, Boynton Beach, FL, USA) was employed. This measurement involved the adsorption of  $\text{N}_2$ , which possesses a molecular surface area of 0.162  $\text{nm}^2$ .

To analyze powdered biochar samples, Fourier-transform infrared (FTIR) analysis was conducted using a PerkinElmer<sup>®</sup> Spectrum 100 FTIR spectrometer equipped with a Micro-ATR crystal accessory. FTIR spectra were collected within the mid-infrared range spanning from 4000 to 600  $\text{cm}^{-1}$ , employing a spectral resolution of 2  $\text{cm}^{-1}$  and a total of 16 scans. Interpretation of the results was based on the identification of broad bands as established in a prior study [29].

### 2.7. Statistical Analysis

The results presented in this paper were calculated as arithmetic means based on triplicate samples. To assess the comparative effectiveness of various biochars in nitrate adsorption, a one-way ANOVA was performed, followed by a post hoc Tukey's test. Significance was considered at  $p \leq 0.05$  unless stated otherwise. All data analyses were conducted using IBM<sup>®</sup> SPSS<sup>®</sup> Statistics software (Version 28.0).

## 3. Results

### 3.1. Residual COD and SCOD in Treated Wastewater

The characteristics of organic compounds in wool scouring wastewater are heavily influenced by the specific wool being processed. In this study, the average COD in untreated Dorset wastewater was found to be 1408.33 mg/L, while untreated BFL wastewater exhibited an average COD of 1504.67 mg/L. Notably, in Dorset wastewater, approximately 38% of the organic constituents were soluble, equating to 536.00 mg/L; in BFL wastewater, roughly 51% of the organics were soluble, totaling 764.67 mg/L. Over the course of adsorption by biochars treated with various chemical agents, encompassing both soluble and insoluble organic compounds, there was a gradual reduction in residual COD and SCOD in the wastewater, reaching equilibrium, as illustrated in Figure 1.

Regarding Dorset wastewater, the highest COD removal, approximately 26%, was achieved by biochar treated with a KOH solution. In terms of COD removal,  $\text{KMnO}_4$ -treated biochar demonstrated an approximately 22% reduction, followed by biochar treated with  $\text{H}_2\text{SO}_4$  and DI water, which exhibited reductions of 19% and 18%, respectively (Figure 1a). The removal of SCOD exceeded that of COD, with KOH-treated biochar removing approximately 61% of SCOD, followed by  $\text{KMnO}_4$ -treated biochar at 53%,  $\text{H}_2\text{SO}_4$ -treated biochar at 47%, and DI-treated biochar at 39% (Figure 1b).

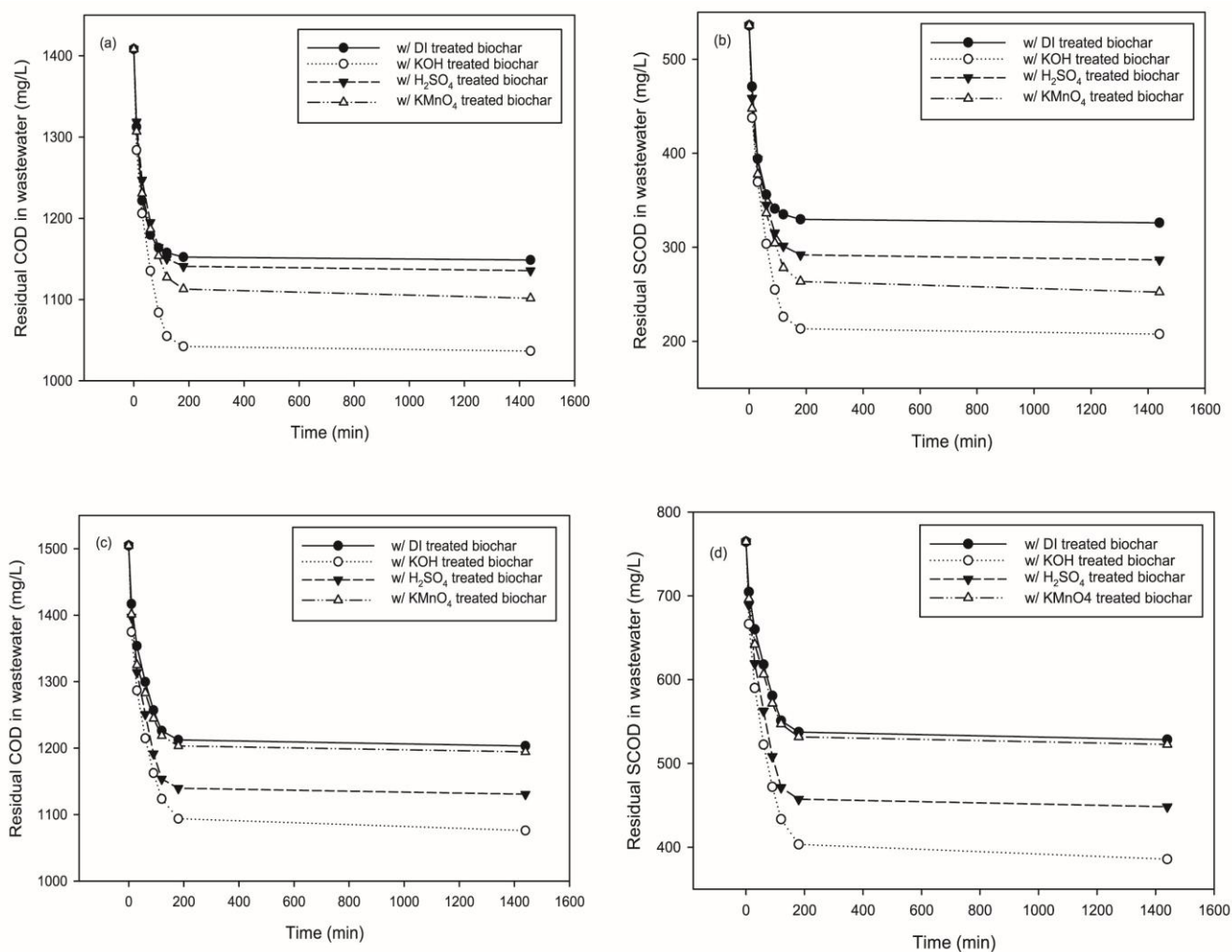


**Figure 1.** Residual COD and soluble COD (SCOD) in wool scouring wastewater treated with biochars modified via different chemical agents: (a) residual COD in Dorset wastewater, (b) residual SCOD in Dorset wastewater, (c) residual COD in BFL wastewater, and (d) residual SCOD in BFL wastewater.

For BFL wastewater, the highest COD removal rate, at 28%, was attained by biochar treated with a KOH solution. In terms of COD removal, H<sub>2</sub>SO<sub>4</sub>-treated biochar exhibited an approximately 25% reduction, followed by biochar treated with KMnO<sub>4</sub> and DI water, with reductions of 21% and 20%, respectively (Figure 1c). Similarly, the removal of SCOD exceeded that of COD, with KOH-treated biochar removing approximately 50% of SCOD, followed by H<sub>2</sub>SO<sub>4</sub>-treated biochar at 41%, KMnO<sub>4</sub>-treated biochar at 32%, and DI-treated biochar at 31% (Figure 1d).

Biochar's enhanced adsorption of soluble organic constituents compared to insoluble ones can be attributed to several factors. First, biochar possesses a highly porous structure with a significant surface area, providing ample adsorption sites for soluble organic molecules [27]. These pores can accommodate and trap smaller, dissolved organic compounds effectively [30]. As stated in a recent study by Tan et al. (2021), the porous nature of biochar contributes significantly to its adsorption capacity for dissolved organics [30]. The porous structure of biochar may restrict the entry of larger, insoluble organic particles, limiting their adsorption. In contrast, soluble organics, being smaller in size, can access and occupy the pores more readily [13]. Second, biochar's surface often contains functional groups such as oxygen-containing moieties (e.g., hydroxyl, carboxyl, and phenolic groups) that can form hydrogen bonds and other attractive interactions with soluble organic compounds [31]. This was discussed in a study by Quan et al. (2020), which emphasized the importance of functional groups in biochar's affinity for dissolved organics [31]. Third,

soluble organic compounds typically carry charged functional groups, making them more susceptible to electrostatic interactions with charged sites on the biochar surface [32]. This concept is highlighted in research by Liu et al. (2018), where electrostatic interactions were identified as a significant factor in the adsorption of soluble organic matter [33].

### 3.2. Removal of COD and SCOD from Wool Scouring Wastewater

As shown in Figure 2, the removal efficiency of both soluble and insoluble organic constituents from wool scouring wastewater increased gradually over time for all the biochars employed in this study. Notably, biochar treated with KOH exhibited the highest effectiveness in removing both COD and SCOD, followed by biochars treated with  $\text{KMnO}_4$ , and then  $\text{H}_2\text{SO}_4$  for Dorset wastewater (Figure 2a,b). Similarly, for BFL wastewater, the order of effectiveness was observed as  $\text{H}_2\text{SO}_4$ -treated biochar,  $\text{KMnO}_4$ -treated biochar, and then DI water-treated biochar (Figure 2c,d).

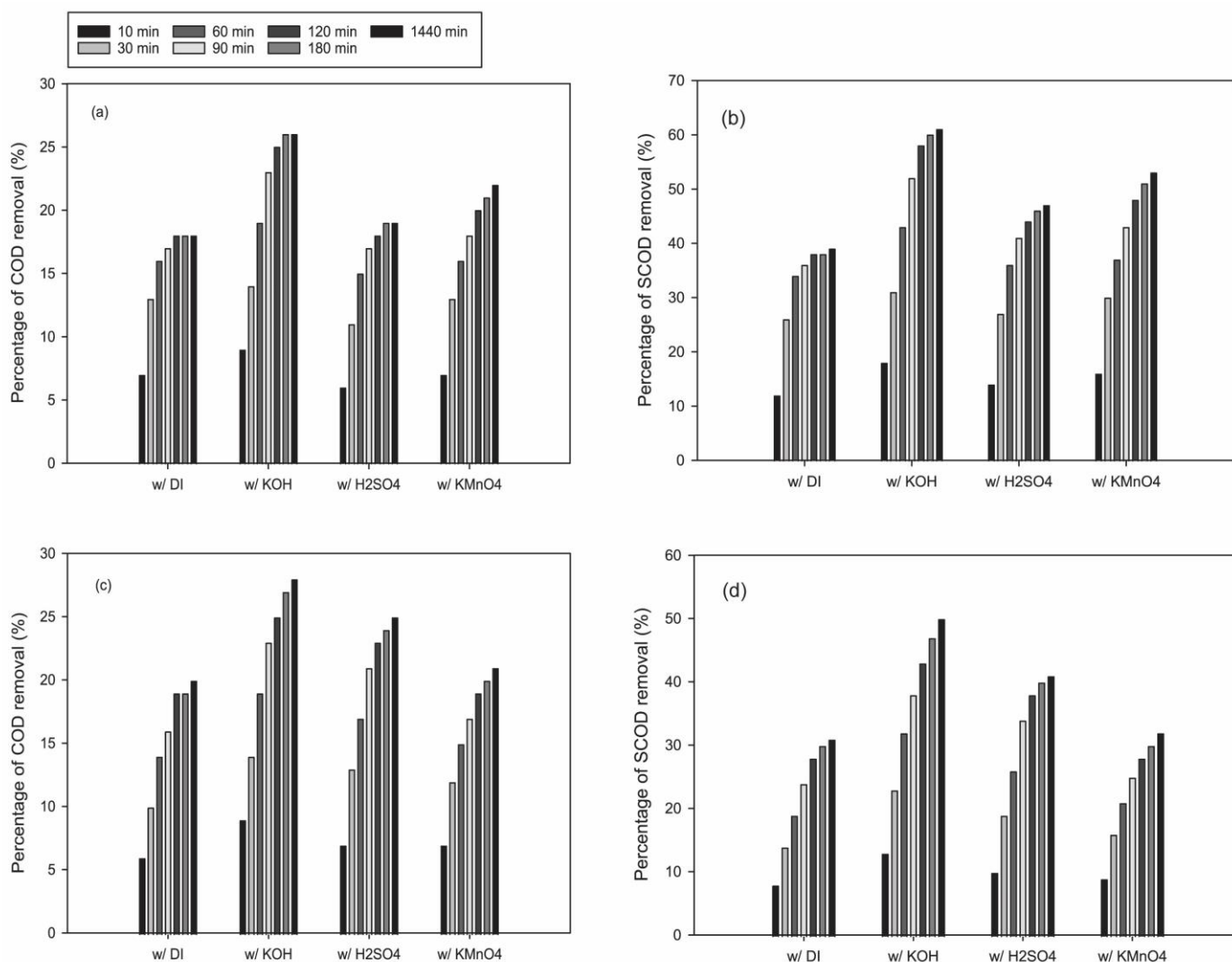


**Figure 2.** Removal rates of COD and SCOD in wool scouring wastewater treated with biochars modified via different chemical agents: (a) residual COD in Dorset wastewater, (b) residual SCOD in Dorset wastewater, (c) residual COD in BFL wastewater, and (d) residual SCOD in BFL wastewater.

The enhanced performance of KOH-treated biochar can be attributed to several key factors. KOH treatment introduces or augments the presence of surface functional groups, such as hydroxyl (-OH) and carboxyl (-COOH) moieties, on the biochar's surface [34]. These functional groups enable the formation of robust hydrogen bonds with soluble organic

compounds, thereby facilitating their adsorption [34]. As demonstrated in a study by Zhao et al. (2020), KOH activation significantly elevates the abundance of surface functional groups on biochar, leading to improved organic contaminant adsorption [35]. Moreover, KOH activation can significantly increase the surface area and porosity of biochar, creating more active sites for organic molecule interactions. This increased surface area provides more opportunities for adsorption [36]. Research by Herath et al. (2021) found that KOH activation led to a substantial increase in the specific surface area of Douglas fir biochar from 535 to 1050 m<sup>2</sup>/g [37]. A study by Jin et al. (2014) highlighted that KOH activation led to a substantial increase in pore volume by nearly 10 times, enhancing the adsorption capacity [38]. KOH activation can modify the surface charge of biochar, making it more favorable for adsorbing organic compounds [39]. Biochar with increased negative surface charge can attract and bind positively charged organic molecules [39]. Jawad et al. (2021) reported that KOH-treated biochar exhibited a more negative surface charge than untreated biochar [40]. Finally, the chemical changes induced by KOH treatment may increase the biochar's affinity for specific organic pollutants. Research by Yang et al. (2018) found that KOH activation modified the surface chemistry of biochar, leading to improved adsorption of selected organic contaminants [41].

Likewise, the application of H<sub>2</sub>SO<sub>4</sub> treatment can introduce or augment the presence of surface functional groups on biochar, potentially including the incorporation of acidic functional groups such as carboxyl (-COOH) and sulfonic (-SO<sub>3</sub>H) moieties [42]. These functional groups have the capacity to enhance biochar's interaction and adsorption capabilities for both organic and inorganic compounds, primarily through electrostatic interactions and chemical bonding [30]. The introduction of acidic functional groups also imparts increased reactivity to the biochar, particularly in applications targeting specific adsorption tasks like the removal of heavy metals or organic contaminants [43]. The alterations in surface characteristics induced by H<sub>2</sub>SO<sub>4</sub> treatment yield a biochar that may exhibit varied affinities for specific compounds [44]. For instance, it could become more efficient at adsorbing particular organic pollutants or heavy metals that display an inclination for acidic functional groups [44]. Furthermore, the treatment can result in an expansion of the specific surface area and porosity of the biochar [45]. This is a consequence of the acid's interaction with the carbonaceous structure, which generates additional micropores and augments the overall surface area accessible for adsorption [45]. As a result, the biochar's adsorption capacity for diverse OFG molecules is notably enhanced. Similarly, owing to the potent oxidative potential of KMnO<sub>4</sub>, post-treatment of biochar with KMnO<sub>4</sub> can also induce noteworthy alterations in its surface characteristics and properties, thereby instigating shifts in its behavior as an adsorbent [25,26].

### 3.3. Adsorption Kinetics

The investigation of adsorption kinetics plays a pivotal role in the treatment of aqueous effluents using biochar adsorption, as it offers crucial insights into the reaction pathways and mechanisms underlying the adsorption processes [46]. In this study, the experimental data were subjected to fitting with the pseudo-first-order kinetic adsorption model (Equation (1)) [47]:

$$\frac{dq}{dt} = k_f \cdot (q_e - q_t) \quad (1)$$

where  $q_t$  is the amount of adsorbate adsorbed at time  $t$  (mg/g),  $q_e$  is the equilibrium adsorption capacity (mg/g),  $k_f$  is the pseudo-first-order rate constant (min<sup>-1</sup>), and  $t$  is the contact time (min).

The integration of Equation (1) with initial conditions,  $q_t = 0$  at  $t = 0$  and  $q_t = q_t$  at  $t = t$ , derives:

$$\ln(q_e - q_t) = \ln(q_e) - k_f \cdot t \quad (2)$$

A nonlinear rearrangement of Equation (2) gives the following:

$$q_t = q_e \cdot [1 - \exp(-k_f \cdot t)] \quad (3)$$

As depicted in Figure 3, the experimental data regarding the adsorption of both COD and SCOD exhibited a strong concordance with the pseudo-first-order kinetic adsorption model. Across both Dorset and BFL wastewaters, the KOH-treated biochar exhibited the highest equilibrium adsorption capacities ( $q_e$ ) for both COD and SCOD. Notably, equilibrium adsorption was achieved within approximately 200 min across the various biochars employed in the treatment of these distinct wool scouring wastewaters. This suggests that an HRT, or the contact time between wastewater and biochar, exceeding 4 h would be unnecessary, as the adsorption process occurred rapidly.

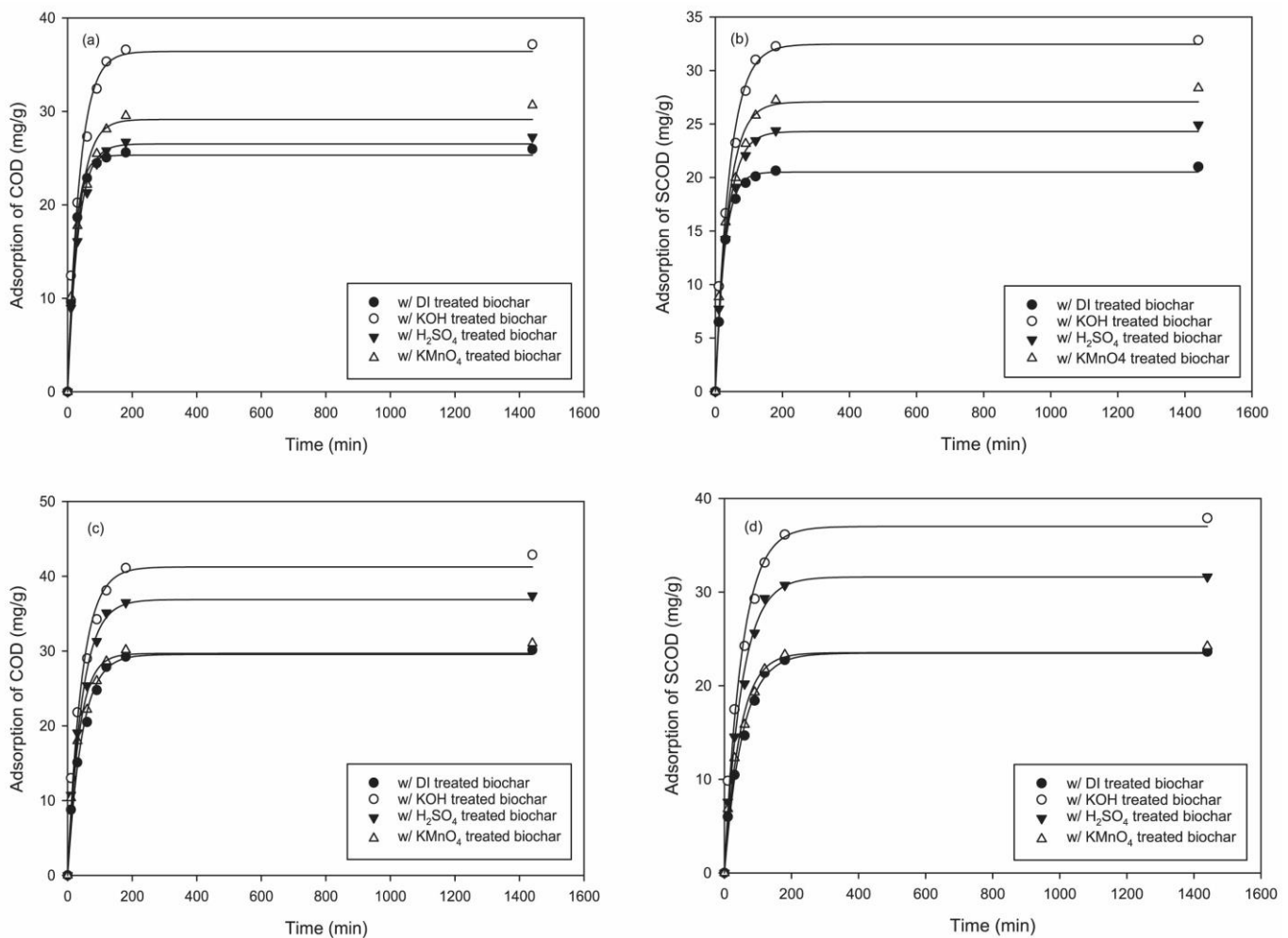


**Figure 3.** Adsorption kinetics of COD and SCOD in wool scouring wastewater treated with biochars modified via different chemical agents: (a) residual COD in Dorset wastewater, (b) residual SCOD in Dorset wastewater, (c) residual COD in BFL wastewater, and (d) residual SCOD in BFL wastewater. The unit “mg/g” denotes the quantity of COD or soluble COD in milligram (mg) removed per gram (g) of adsorbent (biochar) through the adsorption process.

The pseudo-first-order rate constant ( $k_f$ ) serves as an indicator of adsorption intensity, reflecting the rate at which biochar reaches its adsorption equilibrium [47]. The strength of interaction between the adsorbent and adsorbate plays a crucial role. Stronger interactions, such as chemical bonding or electrostatic attraction, can result in a higher  $k_f$  value as they promote rapid adsorption [47]. For Dorset wastewater, biochar treated with DI water

exhibited the highest  $k_f$  value, signifying a swift adsorption process. Conversely, in the case of BFL wastewater, biochar treated with  $\text{KMnO}_4$  displayed the highest  $k_f$  value, suggesting a relatively faster adsorption rate for the interaction between organic contaminants and  $\text{KMnO}_4$ -treated biochar. A comprehensive summary of the parameters derived from the curve fittings is provided in Table 1.

**Table 1.** Adsorption parameters derived from the curve fittings using the pseudo-first-order kinetic adsorption model.

Wastewater	Contaminant Type	Parameters	DI Water Biochar	KOH Biochar	H2SO4 Biochar	KMnO4 Biochar
Dorset	COD	$q_e$ (mg/g)	25.318	36.419	26.520	29.150
Dorset	COD	$k_f$ (min <sup>-1</sup> )	0.0444	0.0272	0.0312	0.0292
Dorset	COD	R2	0.9977	0.9843	0.9917	0.9789
Dorset	SCOD	$q_e$ (mg/g)	20.524	32.460	24.307	27.076
Dorset	SCOD	$k_f$ (min <sup>-1</sup> )	0.0376	0.0239	0.0290	0.0266
Dorset	SCOD	R2	0.9985	0.9885	0.9927	0.9802
BFL	COD	$q_e$ (mg/g)	29.538	41.238	36.878	29.672
BFL	COD	$k_f$ (min <sup>-1</sup> )	0.0226	0.0231	0.0228	0.0286
BFL	COD	R2	0.9861	0.9798	0.9869	0.9778
BFL	SCOD	$q_e$ (mg/g)	23.466	37.012	31.611	23.522
BFL	SCOD	$k_f$ (min <sup>-1</sup> )	0.0185	0.0194	0.0194	0.0218
BFL	SCOD	R2	0.9880	0.9872	0.9921	0.9825

### 3.4. Surface Functional Groups of Biochar

The FTIR spectra of the four biochars were recorded within the range of 400–4000  $\text{cm}^{-1}$ , as illustrated in Figure 4. During the pyrolysis process, the carbonization of components induced an upward shift in the baseline at higher wavenumbers, associated with low-energy electron extractions from condensed aromatic structures. Medium sharp bands spanning the wavenumber range of 3584–3700  $\text{cm}^{-1}$ , as well as weak, broad bands in the range of 2700–3200  $\text{cm}^{-1}$ , were attributed to O-H stretching in various alcohols. Additionally, the presence of strong, broad bands between 3200–3550  $\text{cm}^{-1}$  and 2800–3000  $\text{cm}^{-1}$  was indicative of N-H stretching in different amines. Previous studies have noted that hydroxyl and amino groups within these spectral ranges can enhance the adsorption of fatty organic molecules [48–50], which are prevalent constituents in wool scouring wastewater.

The pronounced bands observed around 1760  $\text{cm}^{-1}$  and within the range of 1680–1720  $\text{cm}^{-1}$  are attributed to the C=O stretching vibrations of various carboxylic acids and conjugated acids. Meanwhile, the moderate bands spanning the 1330 to 1440  $\text{cm}^{-1}$  range are likely a consequence of O-H bending in alcohols, carboxylic acids, and sulfonic acids. These functional groups exhibit a robust affinity for different fats and oils commonly found in wool scouring wastewater. Notably, the changes in surface functional groups within these spectral ranges were particularly significant in  $\text{KMnO}_4$ -treated biochar compared to other biochars.

The introduction or augmentation of surface functional groups on biochar has the potential to enhance its interaction and adsorption capabilities for both organic and inorganic compounds, primarily through electrostatic interactions and chemical bonding [22,43]. The inclusion of acidic functional groups imparts heightened reactivity to the biochar, particularly in applications targeting specific adsorption tasks, such as the removal of OFG molecules [51,52]. However, it is important to acknowledge that the adsorption of contaminants is also profoundly influenced by various other physicochemical properties of biochar [53]. Additionally, due to the chemical's interaction with the carbonaceous structure of biochar, resulting in the generation of additional micropores and an increase in the overall surface area available for adsorption, biochar may experience an expansion of its specific surface area and porosity [13,22,30]. These enhancements significantly augment biochar's adsorption capacity for a wide array of contaminants.

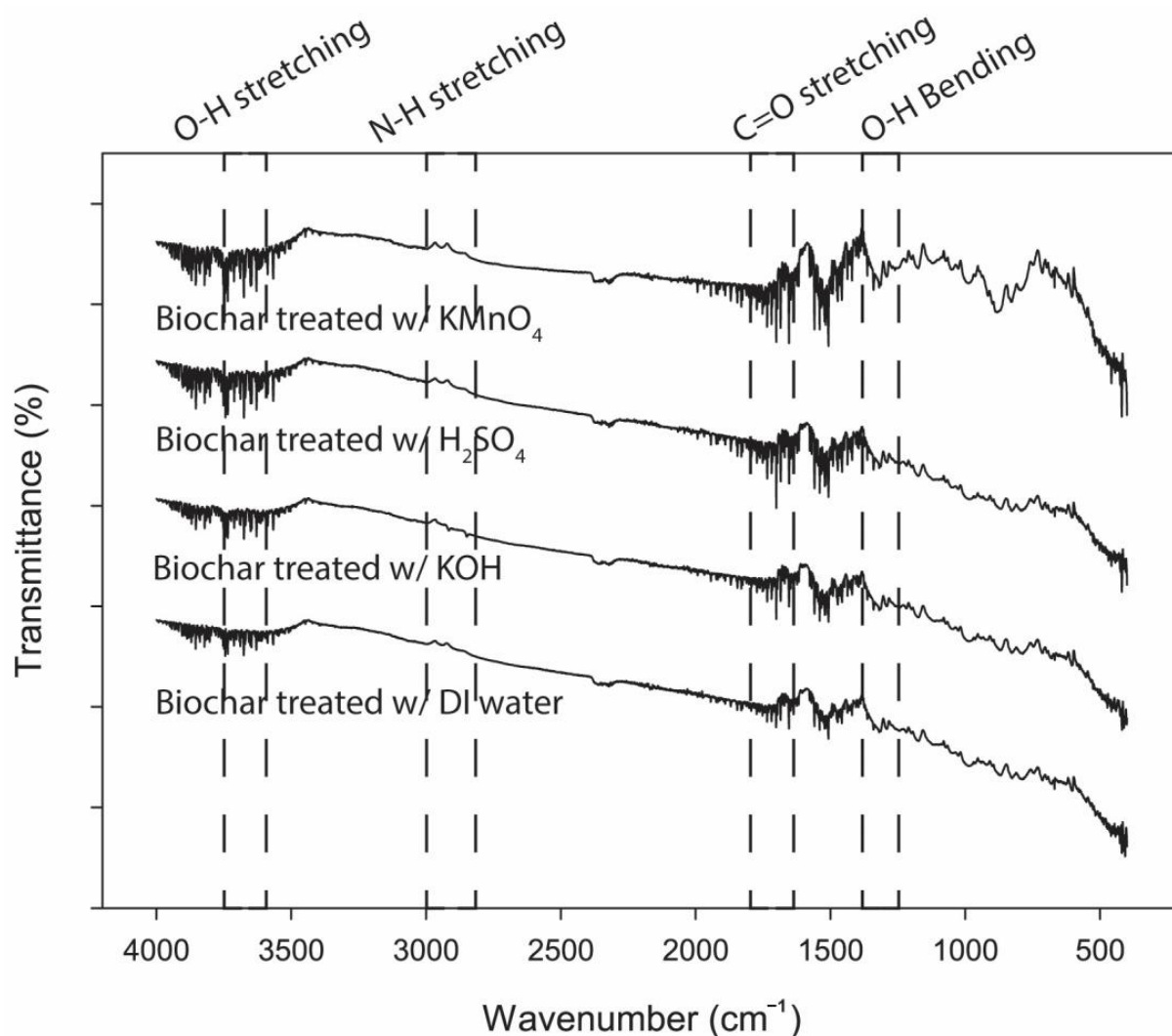


**Figure 4.** Characterization of surface functional groups on biochars treated with various chemical agents using Fourier-transform infrared spectroscopy (FTIR).

### 3.5. Surface Area and Pore Properties of Biochar

As shown in Table 2, the specific surface area of KOH-treated biochar was the highest ( $724.4 \text{ m}^2/\text{g}$ ), followed by  $\text{H}_2\text{SO}_4$ -treated biochar ( $339.2 \text{ m}^2/\text{g}$ ),  $\text{KMnO}_4$  treated biochar ( $238.7 \text{ m}^2/\text{g}$ ), and DI water treated biochar ( $24.6 \text{ m}^2/\text{g}$ ). A larger surface area provides more available adsorption sites on the biochar. Organic contaminants such as oils, fats, and grease can physically adhere to these sites, allowing for a higher quantity of contaminants to be captured and retained by the adsorbent [52,54]. At the same time, a greater surface area enables increased contact between the biochar and the organic contaminants present in the wastewater. This increased contact promotes mass transfer, facilitating the movement of OFG molecules from the liquid phase to the solid phase of the biochar [55]. Moreover, the increased surface area allows for stronger Van der Waals forces, which are attractive forces between nonpolar molecules [56]. OFG molecules, which are typically nonpolar, can be strongly attracted to the biochar surface, enhancing their adsorption [54]. In addition, OFG molecules are often hydrophobic (water-repellent). A large specific surface area with a high hydrophobicity can preferentially adsorb hydrophobic OFG compounds, as the biochar provides an environment more favorable to these compounds than the aqueous phase [57].

**Table 2.** Surface area and pore properties of biochar.

	BET Surface Area (m <sup>2</sup> /g)	Micropore (<2 nm)	Mesopore (2–50 nm)	Macropore (>50 nm)	Total Pore Volume (cm <sup>3</sup> /g)
DI water-treated biochar	24.6	14%	71%	15%	0.062
KOH-treated biochar	724.4	94%	4%	2%	0.746
H <sub>2</sub> SO <sub>4</sub> -treated biochar	339.2	39%	48%	13%	1.061
KMnO <sub>4</sub> -treated biochar	238.7	78%	20%	1%	0.224

A large specific surface area is often associated with a greater pore volume, including mesopores and micropores [56]. These pores provide additional space for the adsorption of OFG molecules. Micropores, in particular, can adsorb organic molecules effectively due to their small size and high surface area [33]. The pore distributions of biochars treated with different chemical agents varied significantly [56]. For example, KOH-treated biochar had 94% micropores (<2 nm), while DI water-treated biochar had only 14% micropores. Smaller pores within the biochar can generate capillary forces, which can pull organic contaminants into the pores, effectively trapping them. This capillary action can be especially beneficial for capturing small OFG droplets or dispersed phases in the wastewater [58]. However, despite their high adsorption capacity, the small size of micropores can lead to diffusion limitations, especially for larger OFG molecules, which may hinder rapid adsorption [59]. Hence, mesopores strike a balance between surface area and accessibility. They offer a moderate surface area for adsorption while allowing relatively easier access for OFG molecules [40]. Mesopores are particularly effective at adsorbing OFG molecules of moderate size [40]. They can capture larger OFG droplets or aggregates while providing a sufficient surface area for adsorption [55]. Compared to micropores, mesopores often allow for faster mass transfer of OFG molecules, resulting in quicker adsorption kinetics. Meanwhile, macropores themselves may not directly adsorb OFG molecules due to their larger size. Instead, they can serve as channels or conduits for the movement of OFG-contaminated water through the biochar [59].

### 3.6. Proximate and Elemental Analysis of Biochar

Table 3 presents a comprehensive proximate analysis of various biochars, offering valuable insights into their composition and properties, which play pivotal roles in their effectiveness as adsorbents for the removal of organic contaminants from wastewater.

**Table 3.** Proximate analysis and elemental composition of biochar.

	Volatile Matter	Fixed Carbon	Ash	C	H	O	N	S
DI water treated biochar	57.31%	34.03%	8.66%	74.52%	4.43%	9.81%	2.56%	0.02%
KOH treated biochar	40.73%	49.58%	9.69%	81.53%	2.88%	3.23%	2.64%	0.03%
H <sub>2</sub> SO <sub>4</sub> treated biochar	43.87%	51.31%	4.82%	91.32%	1.58%	1.66%	0.53%	0.09%
KMnO <sub>4</sub> treated biochar	52.15%	40.38%	7.47%	84.61%	2.53%	4.31%	1.03%	0.05%

Notably, the volatile matter content stands out as a differentiating factor among the examined biochars. The DI water-treated biochar records the highest volatile matter content at 57.31%, signifying a greater proportion of materials that can readily vaporize at elevated temperatures. In stark contrast, the KOH-treated biochar exhibits the lowest volatile matter content at 40.73%, indicative of a more resilient and carbon-rich structure [60]. This enhanced stability holds the potential to provide an expanded surface area and heightened adsorption capacity [19], particularly for hydrophobic OFG compounds.

Furthermore, fixed carbon content emerges as a critical parameter in delineating biochar efficacy [60]. Biochars characterized by higher fixed carbon content, exemplified by the KOH-treated and H<sub>2</sub>SO<sub>4</sub>-treated variants, signify a larger share of carbonaceous material that endures post-pyrolysis [29]. Such a carbon-rich framework enhances their

suitability as OFG adsorbents, given that stable carbon structures yield abundant adsorption sites.

Ash content, serving as a proxy for inorganic mineral content, can exert a tangible influence on the adsorption prowess of biochar [39]. The preference generally leans toward lower ash content, as seen in the KOH-treated biochar, as it ensures a more substantial surface area available for OFG adsorption.

Examining the elemental composition (C, H, O, N, S) underscores variations in the chemical makeup of the biochars. For instance, KOH-treated biochar showcases the highest carbon (C) content at 81.53%, while H<sub>2</sub>SO<sub>4</sub>-treated biochar boasts the highest hydrogen (H) content at 2.88%. These disparities in elemental composition can profoundly affect the interactions between biochar and OFG molecules, involving electrostatic attractions and chemical bonding [53].

In sum, proximate analysis outcomes illuminate KOH-treated biochar as a standout candidate for OFG removal. With its lower volatile matter, higher fixed carbon content, and reduced ash content, it portrays a stable, carbon-rich architecture that holds great promise for efficient adsorption of hydrophobic OFG compounds. Nevertheless, a comprehensive evaluation of each biochar's suitability for OFG removal necessitates consideration of additional factors such as surface area and pore characteristics [53].

#### 4. Conclusions

This study assessed the efficacy of various chemically modified biochars in the removal of oils, fats, and grease (OFG) from wool scouring wastewater. Proximate analysis unveiled distinct biochar properties, with KOH-treated biochar emerging as a promising choice due to its lower volatile matter, higher fixed carbon content, and reduced ash content. These attributes indicate a stable, carbon-rich structure conducive to the efficient adsorption of hydrophobic OFG compounds. Our investigation successfully modeled the adsorption kinetics of chemical oxygen demand (COD) and soluble COD (SCOD) using the pseudo-first-order kinetic model. Equilibrium was attained within approximately 200 min, with KOH-treated biochar demonstrating the highest equilibrium adsorption capacities for both COD and SCOD in both Dorset and BFL wastewater, underscoring its effectiveness in OFG removal.

Nonetheless, it is vital to acknowledge this study's limitations. Primarily focusing on kinetic adsorption aspects, there remains room for further exploration of biochar's surface characteristics, pore structure, and performance under diverse conditions. Field-scale investigations and long-term stability assessments in practical applications are essential to ascertain real-world feasibility. Future research avenues include expanding the scope to encompass a broader range of chemical modifications, diverse wastewater sources, and optimization of operational parameters. Additionally, investigating biochar's regeneration potential, its integration with existing treatment methods, and its suitability for reuse can enhance sustainability and practical applicability in wastewater treatment processes.

**Author Contributions:** Conceptualization, S.L.; methodology, S.L., D.T. and B.C.; software, S.L.; validation, D.T., S.S. and B.C.; formal analysis, S.L. and B.C.; investigation, D.T., S.S., B.C. and S.J.; resources, S.L.; data curation, D.T., S.S., B.C. and S.J.; writing—original draft preparation, S.L.; writing—review and editing, D.T. and S.S.; visualization, S.L. and B.C.; supervision, S.L.; project administration, S.L.; funding acquisition, S.L. All authors have read and agreed to the published version of the manuscript.

**Funding:** This research was funded by USDA-NIFA, HSI Education Program, grant number 2020-38422-32253.

**Data Availability Statement:** The data presented in this study are available on request from the corresponding author.

**Acknowledgments:** The authors are grateful for the donation of wool samples by Helen X. Trejo, Department of Apparel Merchandising and Management, California State Polytechnic University, Pomona.

**Conflicts of Interest:** The authors declare no conflicts of interest. The funders had no role in the design of the study; in the collection, analyses, or interpretation of data; in the writing of the manuscript; or in the decision to publish the results.

## References

1. Bhavsar, P.; Zoccola, M.; Dalla Fontana, G.; Pallavicini, M.; Roda, G.; Bolchi, C. Sustainable Routes for Wool Grease Removal Using Green Solvent Cyclopentyl Methyl Ether in Solvent Extraction and Biosurfactant Wool Protein Hydrolyzate in Scouring. *Processes* **2023**, *11*, 1309. [[CrossRef](#)]
2. Lin, Y.; Hao, Z.; Liu, J.; Han, J.; Wang, A.; Ouyang, Q.; Fu, F. Molecular probing of dissolved organic matter and its transformation in a woolen textile wastewater treatment station. *J. Hazard. Mater.* **2023**, *457*, 131807. [[CrossRef](#)]
3. Allafi, F.A.; Hossain, M.S.; Shaah, M.; Lalung, J.; Ab Kadir, M.O.; Ahmad, M.I. A review on characterization of sheep wool impurities and existing techniques of cleaning: Industrial and environmental challenges. *J. Nat. Fibers* **2022**, *19*, 8669–8687. [[CrossRef](#)]
4. Chaupin, M. Wool Scouring in Europe: Urgent and Ecological Solutions. In *Advances in Fibre Production Science in South American Camelids and Other Fibre Animals*; Gerken, M., Renieri, C., Allain, D., Galbraith, H., Gutiérrez, J.P., McKenna, L., Niznikowski, R., Wurzinger, M., Eds.; Universitätsverlag Göttingen: Göttingen, Germany, 2019; p. 301.
5. Saran, R.K.; Kumar, R.; Yadav, S. Environmental issues in textiles. In *Advanced Functional Textiles and Polymers: Fabrication, Processing and Applications*; Wiley-Scrivener: Austin, TX, USA, 2019; pp. 129–151.
6. Awchat, G.D. Upgradation of wool scouring plant for efficient wastewater treatment. *Ecol. Eng. Environ. Technol.* **2022**, *23*, 11–18. [[CrossRef](#)] [[PubMed](#)]
7. Pattnaik, P.; Dangayach, G.S. Sustainability of wastewater management in textile sectors: A conceptual framework. *Environ. Eng. Manag. J.* **2019**, *18*, 1947–1965. [[CrossRef](#)]
8. Shanmugasundaram, O.; Pandit, P. Conclusion on biotechnology in textile production and future scope. In *Applications of Biotechnology for Sustainable Textile Production*; Elsevier: Amsterdam, The Netherlands, 2022; pp. 241–249.
9. Shi, C.; Wang, Q.; Li, D.; Zeng, B.; Liu, Q.; Cui, Y.; Wang, J.; Wang, X. Inorganic composite coagulant for wool scouring wastewater treatment: Performance, kinetics and coagulation mechanism. *Sep. Purif. Technol.* **2023**, *313*, 123482. [[CrossRef](#)]
10. Iwuozor, K.O. Prospects and challenges of using coagulation-flocculation method in the treatment of effluents. *Adv. J. Chem. Sect. A* **2019**, *2*, 105–127. [[CrossRef](#)]
11. Cinperi, N.C.; Ozturk, E.; Yigit, N.O.; Kitis, M. Treatment of woolen textile wastewater using membrane bioreactor, nanofiltration and reverse osmosis for reuse in production processes. *J. Clean. Prod.* **2019**, *223*, 837–848. [[CrossRef](#)]
12. Ahmad, N.N.R.; Ang, W.L.; Teow, Y.H.; Mohammad, A.W.; Hilal, N. Nanofiltration membrane processes for water recycling, reuse and product recovery within various industries: A review. *J. Water Process Eng.* **2022**, *45*, 102478. [[CrossRef](#)]
13. Ou, S.-F.; Yang, D.-S.; Liao, J.-W.; Chen, S.-T. Treating high COD dyeing wastewater via a regenerative sorption-oxidation process using a nano-pored activated carbon. *Int. J. Mol. Sci.* **2022**, *23*, 4752. [[CrossRef](#)]
14. Li, R.; Wang, B.; Niu, A.; Cheng, N.; Chen, M.; Zhang, X.; Yu, Z.; Wang, S. Application of biochar immobilized microorganisms for pollutants removal from wastewater: A review. *Sci. Total Environ.* **2022**, *837*, 155563. [[CrossRef](#)] [[PubMed](#)]
15. Li, S.; Chan, C.Y.; Sharbatmaleki, M.; Trejo, H.; Delagah, S. Engineered Biochar Production and Its Potential Benefits in a Closed-Loop Water-Reuse Agriculture System. *Water* **2020**, *12*, 2847. [[CrossRef](#)]
16. Lotito, A.M.; De Sanctis, M.; Di Iaconi, C.; Bergna, G. Textile wastewater treatment: Aerobic granular sludge vs activated sludge systems. *Water Res.* **2014**, *54*, 337–346. [[CrossRef](#)] [[PubMed](#)]
17. Brickler, C.A.; Wu, Y.; Li, S.; Anandhi, A.; Chen, G. Comparing Physicochemical Properties and Sorption Behaviors of Pyrolysis-Derived and Microwave-Mediated Biochar. *Sustainability* **2021**, *13*, 2359. [[CrossRef](#)]
18. Li, S.; Skelly, S. Physicochemical properties and applications of biochars derived from municipal solid waste: A review. *Environ. Adv.* **2023**, *13*, 100395. [[CrossRef](#)]
19. Li, S.; Galoustian, T.; Trejo, H. Biochar pyrolyzed with concentrated solar radiation for enhanced nitrate adsorption. *J. Anal. Appl. Pyrolysis* **2023**, *174*, 106131. [[CrossRef](#)]
20. Tomczyk, A.; Kondracki, B.; Szewczuk-Karpisz, K. Chemical modification of biochars as a method to improve its surface properties and efficiency in removing xenobiotics from aqueous media. *Chemosphere* **2023**, *312*, 137238. [[CrossRef](#)]
21. Liu, Z.; Xu, Z.; Xu, L.; Buyong, F.; Chay, T.C.; Li, Z.; Cai, Y.; Hu, B.; Zhu, Y.; Wang, X. Modified biochar: Synthesis and mechanism for removal of environmental heavy metals. *Carbon Res.* **2022**, *1*, 8. [[CrossRef](#)]
22. Fahmi, A.H.; Jol, H.; Singh, D. Physical modification of biochar to expose the inner pores and their functional groups to enhance lead adsorption. *RSC Adv.* **2018**, *8*, 38270–38280. [[CrossRef](#)]
23. Xie, Y.; Wang, L.; Li, H.; Westholm, L.J.; Carvalho, L.; Thorin, E.; Yu, Z.; Yu, X.; Skreiberg, Ø. A critical review on production, modification and utilization of biochar. *J. Anal. Appl. Pyrolysis* **2022**, *161*, 105405. [[CrossRef](#)]
24. Fan, Z.; Zhang, Q.; Li, M.; Niu, D.; Sang, W.; Verpoort, F. Investigating the sorption behavior of cadmium from aqueous solution by potassium permanganate-modified biochar: Quantify mechanism and evaluate the modification method. *Environ. Sci. Pollut. Res.* **2018**, *25*, 8330–8339. [[CrossRef](#)]

25. Zheng, Y.; Wang, J.; Li, D.; Liu, C.; Lu, Y.; Lin, X.; Zheng, Z. Insight into the KOH/KMnO<sub>4</sub> activation mechanism of oxygen-enriched hierarchical porous biochar derived from biomass waste by in-situ pyrolysis for methylene blue enhanced adsorption. *J. Anal. Appl. Pyrolysis* **2021**, *158*, 105269. [[CrossRef](#)]
26. Huang, Z.; Fang, X.; Wang, S.; Zhou, N.; Fan, S. Effects of KMnO<sub>4</sub> pre-and post-treatments on biochar properties and its adsorption of tetracycline. *J. Mol. Liq.* **2023**, *373*, 121257. [[CrossRef](#)]
27. Li, R.; Wang, Z.; Guo, J.; Li, Y.; Zhang, H.; Zhu, J.; Xie, X. Enhanced adsorption of ciprofloxacin by KOH modified biochar derived from potato stems and leaves. *Water Sci. Technol.* **2018**, *77*, 1127–1136. [[CrossRef](#)] [[PubMed](#)]
28. Qi, Y.; Zhong, Y.; Luo, L.; He, J.; Feng, B.; Wei, Q.; Zhang, K.; Ren, H. Subsurface constructed wetlands with modified biochar added for advanced treatment of tailwater: Performance and microbial communities. *Sci. Total Environ.* **2024**, *906*, 167533. [[CrossRef](#)] [[PubMed](#)]
29. Li, S.; Chen, G. Thermogravimetric, thermochemical, and infrared spectral characterization of feedstocks and biochar derived at different pyrolysis temperatures. *Waste Manag.* **2018**, *78*, 198–207. [[CrossRef](#)] [[PubMed](#)]
30. Tan, X.-F.; Zhu, S.-S.; Wang, R.-P.; Chen, Y.-D.; Show, P.-L.; Zhang, F.-F.; Ho, S.-H. Role of biochar surface characteristics in the adsorption of aromatic compounds: Pore structure and functional groups. *Chin. Chem. Lett.* **2021**, *32*, 2939–2946. [[CrossRef](#)]
31. Quan, G.; Fan, Q.; Zimmerman, A.R.; Sun, J.; Cui, L.; Wang, H.; Gao, B.; Yan, J. Effects of laboratory biotic aging on the characteristics of biochar and its water-soluble organic products. *J. Hazard. Mater.* **2020**, *382*, 121071. [[CrossRef](#)]
32. Yakout, S.M. Monitoring the changes of chemical properties of rice straw-derived biochars modified by different oxidizing agents and their adsorptive performance for organics. *Bioremediation J.* **2015**, *19*, 171–182. [[CrossRef](#)]
33. Liu, G.; Zheng, H.; Zhai, X.; Wang, Z. Characteristics and mechanisms of microcystin-LR adsorption by giant reed-derived biochars: Role of minerals, pores, and functional groups. *J. Clean. Prod.* **2018**, *176*, 463–473. [[CrossRef](#)]
34. Kumar, A.; Bhattacharya, T.; Shaikh, W.A.; Chakraborty, S.; Sarkar, D.; Biswas, J.K. Biochar modification methods for augmenting sorption of contaminants. *Curr. Pollut. Rep.* **2022**, *8*, 519–555. [[CrossRef](#)]
35. Zhao, C.; Ma, J.; Li, Z.; Xia, H.; Liu, H.; Yang, Y. Highly enhanced adsorption performance of tetracycline antibiotics on KOH-activated biochar derived from reed plants. *RSC Adv.* **2020**, *10*, 5066–5076. [[CrossRef](#)] [[PubMed](#)]
36. Li, Y.; Wang, B.; Shang, H.; Cao, Y.; Yang, C.; Hu, W.; Feng, Y.; Yu, Y. Influence of adsorption sites of biochar on its adsorption performance for sulfamethoxazole. *Chemosphere* **2023**, *326*, 138408. [[CrossRef](#)] [[PubMed](#)]
37. Herath, A.; Layne, C.A.; Perez, F.; Hassan, E.I.B.; Pittman, C.U.; Mlsna, T.E. KOH-activated high surface area Douglas Fir biochar for adsorbing aqueous Cr(VI), Pb(II) and Cd(II). *Chemosphere* **2021**, *269*, 128409. [[CrossRef](#)] [[PubMed](#)]
38. Jin, H.; Capareda, S.; Chang, Z.; Gao, J.; Xu, Y.; Zhang, J. Biochar pyrolytically produced from municipal solid wastes for aqueous As(V) removal: Adsorption property and its improvement with KOH activation. *Bioresour. Technol.* **2014**, *169*, 622–629. [[CrossRef](#)]
39. Bashir, S.; Zhu, J.; Fu, Q.; Hu, H. Comparing the adsorption mechanism of Cd by rice straw pristine and KOH-modified biochar. *Environ. Sci. Pollut. Res.* **2018**, *25*, 11875–11883. [[CrossRef](#)] [[PubMed](#)]
40. Jawad, A.H.; Abdulhameed, A.S.; Wilson, L.D.; Syed-Hassan, S.S.A.; ALOthman, Z.A.; Khan, M.R. High surface area and mesoporous activated carbon from KOH-activated dragon fruit peels for methylene blue dye adsorption: Optimization and mechanism study. *Chin. J. Chem. Eng.* **2021**, *32*, 281–290. [[CrossRef](#)]
41. Yang, K.; Zhu, L.; Yang, J.; Lin, D. Adsorption and correlations of selected aromatic compounds on a KOH-activated carbon with large surface area. *Sci. Total Environ.* **2018**, *618*, 1677–1684. [[CrossRef](#)]
42. Qu, Y.; Xu, L.; Chen, Y.; Sun, S.; Wang, Y.; Guo, L. Efficient toluene adsorption/desorption on biochar derived from in situ acid-treated sugarcane bagasse. *Environ. Sci. Pollut. Res.* **2021**, *28*, 62616–62627. [[CrossRef](#)]
43. Zhang, H.; Yue, X.; Li, F.; Xiao, R.; Zhang, Y.; Gu, D. Preparation of rice straw-derived biochar for efficient cadmium removal by modification of oxygen-containing functional groups. *Sci. Total Environ.* **2018**, *631*, 795–802. [[CrossRef](#)]
44. Rose, P.K.; Kataria, N.; Khoo, K.S.; Narwal, N.; Dhull, S.B.; Kumar, R.; Rani, S.; Kumar, P. Pristine and Modified Biochar for Pharmaceuticals Removal from Aquatic Systems. In *Pharmaceuticals in Aquatic Environments*; CRC Press: Boca Raton, FL, USA, 2024; pp. 145–172.
45. Murtaza, G.; Ahmed, Z.; Usman, M. Feedstock type, pyrolysis temperature and acid modification effects on physicochemical attributes of biochar and soil quality. *Arab. J. Geosci.* **2022**, *15*, 305. [[CrossRef](#)]
46. Tong, Y.; McNamara, P.J.; Mayer, B.K. Adsorption of organic micropollutants onto biochar: A review of relevant kinetics, mechanisms and equilibrium. *Environ. Sci. Water Res. Technol.* **2019**, *5*, 821–838. [[CrossRef](#)]
47. Revellame, E.D.; Fortela, D.L.; Sharp, W.; Hernandez, R.; Zappi, M.E. Adsorption kinetic modeling using pseudo-first order and pseudo-second order rate laws: A review. *Clean. Eng. Technol.* **2020**, *1*, 100032. [[CrossRef](#)]
48. Thomas, M.M.; Clouse, J.A.; Longo, J.M. Adsorption of organic compounds on carbonate minerals: 1. Model compounds and their influence on mineral wettability. *Chem. Geol.* **1993**, *109*, 201–213. [[CrossRef](#)]
49. Atanassova, I.; Doerr, S. Organic compounds of different extractability in total solvent extracts from soils of contrasting water repellency. *Eur. J. Soil Sci.* **2010**, *61*, 298–313. [[CrossRef](#)]
50. Mezzetta, A.; Luczak, J.; Woch, J.; Chiappe, C.; Nowicki, J.; Guazzelli, L. Surface active fatty acid ILs: Influence of the hydrophobic tail and/or the imidazolium hydroxyl functionalization on aggregates formation. *J. Mol. Liq.* **2019**, *289*, 111155. [[CrossRef](#)]
51. Jagadeesh, N.; Sundaram, B. Adsorption of pollutants from wastewater by biochar: A review. *J. Hazard. Mater. Adv.* **2023**, *9*, 100226. [[CrossRef](#)]

52. Ren, H.-Y.; Wei, Z.-J.; Wang, Y.; Deng, Y.-P.; Li, M.-Y.; Wang, B. Effects of biochar properties on the bioremediation of the petroleum-contaminated soil from a shale-gas field. *Environ. Sci. Pollut. Res.* **2020**, *27*, 36427–36438. [[CrossRef](#)]
53. Li, S.; Harris, S.; Anandhi, A.; Chen, G. Predicting biochar properties and functions based on feedstock and pyrolysis temperature: A review and data syntheses. *J. Clean. Prod.* **2019**, *215*, 890–902. [[CrossRef](#)]
54. Gurav, R.; Bhatia, S.K.; Choi, T.-R.; Choi, Y.-K.; Kim, H.J.; Song, H.-S.; Park, S.L.; Lee, H.S.; Lee, S.M.; Choi, K.-Y. Adsorptive removal of crude petroleum oil from water using floating pinewood biochar decorated with coconut oil-derived fatty acids. *Sci. Total Environ.* **2021**, *781*, 146636. [[CrossRef](#)]
55. Das, L.; Sengupta, S.; Das, P.; Bhowal, A.; Bhattacharjee, C. Experimental and Numerical modeling on dye adsorption using pyrolyzed mesoporous biochar in Batch and fixed-bed column reactor: Isotherm, Thermodynamics, Mass transfer, Kinetic analysis. *Surf. Interfaces* **2021**, *23*, 100985. [[CrossRef](#)]
56. Bardestani, R.; Patience, G.S.; Kaliaguine, S. Experimental methods in chemical engineering: Specific surface area and pore size distribution measurements—BET, BJH, and DFT. *Can. J. Chem. Eng.* **2019**, *97*, 2781–2791. [[CrossRef](#)]
57. Zhu, L.; Zhao, N.; Tong, L.; Lv, Y. Structural and adsorption characteristics of potassium carbonate activated biochar. *RSC Adv.* **2018**, *8*, 21012–21019. [[CrossRef](#)] [[PubMed](#)]
58. Mandal, S.; Ishak, S.; Lee, D.-E.; Park, T. Optimization of eco-friendly Pinus resinosa biochar-dodecanoic acid phase change composite for the cleaner environment. *J. Energy Storage* **2022**, *55*, 105414. [[CrossRef](#)]
59. Wan, S.; Qiu, L.; Tang, G.; Chen, W.; Li, Y.; Gao, B.; He, F. Ultrafast sequestration of cadmium and lead from water by manganese oxide supported on a macro-mesoporous biochar. *Chem. Eng. J.* **2020**, *387*, 124095. [[CrossRef](#)]
60. Li, S.; Barreto, V.; Li, R.; Chen, G.; Hsieh, Y.P. Nitrogen retention of biochar derived from different feedstocks at variable pyrolysis temperatures. *J. Anal. Appl. Pyrolysis* **2018**, *133*, 136–146. [[CrossRef](#)]

**Disclaimer/Publisher’s Note:** The statements, opinions and data contained in all publications are solely those of the individual author(s) and contributor(s) and not of MDPI and/or the editor(s). MDPI and/or the editor(s) disclaim responsibility for any injury to people or property resulting from any ideas, methods, instructions or products referred to in the content.